

Dark Sector spectroscopy at the ILC

Jeppe R. Andersen* and Michael Spannowsky†

Institute for Particle Physics Phenomenology, Department of Physics, Durham University, United Kingdom

Michael Rauch‡

Institute for Theoretical Physics, University of Karlsruhe, Germany

Recent studies have shown that searches in the mono-photon and missing energy final state can be used to discover dark matter candidates at the ILC. While an excess in this final state over the Standard Model background would indicate the existence of a dark sector, no detailed information about the internal structure of this sector can be inferred. Here, we demonstrate how just a few observables can discriminate between various realizations of dark sectors, including e.g. the spin of mediators.

PACS numbers:

I. INTRODUCTION

Astronomical observations strongly indicate the existence of dark matter [1]. Many extensions of the Standard-Model take this into account by incorporating a so-called dark sector: a sector of particles that do not carry electric or colour charge. The interactions of the dark sector can be protected by global symmetries and the particles can have a long lifetime. Often the dark sector is not completely decoupled, but interacts with the Standard Model particles by the exchange of a Z boson, or a mediator of a yet unknown force.

In recent years several experiments, i.e. PAMELA [2], Fermi LAT [3] and most recently AMS [4], have observed an excess in the positron fraction in the electron-positron energy spectrum at energies above ~ 10 GeV. A possible explanation for this excess could be the decay of an invisible particle into an e^+e^- pair. Leptophilic dark sectors have been identified as a possible explanation of the observed excess [28–30, 32].

Unfortunately, due to the large uncertainties in evaluating the cosmological backgrounds, indirect detection experiments face challenges in claiming the discovery of a potential dark matter candidate. Direct detection experiments try to measure the momentum transfer between the weakly interacting massive particle (WIMP) and the detector. If the WIMP is light, the sensitivity of the experiments are strongly reduced [5]. Interpretations of searches for WIMPs at direct detection experiments usually assume that the dark sector is minimal, i.e. consists of only one particle, and the WIMP accounts for the total dark matter abundance in the universe. We will not make those strong assumptions. Indeed, if the dark sector is not minimal or the WIMP is not even stable on cosmological time scales constraints from direct detection experiments are strongly relaxed.

Recently it has been pointed out that in case the WIMP couples with reasonable strength to quarks, mono-jet searches at the Tevatron and LHC can be a superior way in discovering them [6–10, 12–15]. If the WIMP couples predominantly to leptons constraints can be derived from LEP in mono-photon searches [16] or a future electron positron collider [34].

Unfortunately both, direct detection experiments and mono-jet/photon searches, are very limited tools in unravelling the detailed structure of the dark sector, e.g. the spin of the force mediator in combination with its mass and the mass of the WIMP(s). In mono-photon searches the WIMPs recoil against a high pT photon. Therefore, only the total amount of missing transverse energy in the event can be measured, i.e. the differential cross section for one observable.

The observables discussed in this article allow an unbiased view into the dark sector, as long as a mediator couples the dark sector to electrons. Because of the lack of an existing electron-positron collider we will discuss these observables in the context of the International Linear Collider (ILC). So far, the ILC's great potential in studying the structure of dark sectors has not been completely appreciated [35]. We assume that the particles in the dark sector are stable on collider time scales and escape detection at the LHC. Therefore, our signal will consist of electrons and missing transverse energy (MET). This signature is relatively rare in the Standard Model, predominantly generated in the production of Z bosons and photons with subsequent decay/splitting to an e^+e^- pair and neutrinos. An important topology for the study of the structure of the dark sector is the so-called vector boson fusion (VBF) topology (i.e., two possibly forward well-separated electrons), even though the dark sector particles are not necessarily produced by exchanging a vector boson. Tight cuts on the electron-positron system can reduce the Standard Model backgrounds and increase the average energy flowing through the WIMPs- e^+e^- coupling. A similar strategy is used when studying the coupling structure of the Higgs boson to quarks: Producing a Higgs boson in the VBF channel, angular correlations of the jets can be used to distin-

*Electronic address: jeppe.andersen@durham.ac.uk

†Electronic address: michael.spannowsky@durham.ac.uk

‡Electronic address: michael.rauch@kit.edu

	scalar	vector
e	$i g_{ee\phi,S} \bar{e}e \phi_S$	$i g_{ee\phi,V} \bar{e}\gamma_\mu e \phi_V^\mu$
χ	$i g_{\chi\chi\phi,S} \bar{\chi}\chi \phi_S$	$i g_{\chi\chi\phi,V} \bar{\chi}\gamma_\mu \chi \phi_V^\mu$

TABLE I: Terms in the Lagrangian describing interactions between the mediator and the electron or the WIMP particle.

guish a CP-even from a CP-odd Higgs boson [17–19] and an invisibly decaying Higgs boson can be disentangled from the backgrounds [20]. Similar kinematic configurations can be used to study dark sectors with WIMP-quark couplings at the LHC. However, we find that at the LHC the WIMP-quark coupling has to be of the order of the electroweak coupling to give a significant event shape contribution, reflected in m_{jj} or Δy_{jj} . Further, at the LHC large systematic uncertainties in final states with missing transverse energy (MET) and jets render a dark sector spectroscopy a difficult task [31].

This article is organized as follows: In section II we discuss our benchmark models and assumptions which specify the WIMPs-electron-positron interactions. Kinematic observables are identified and interpreted in the context of Regge theory in section III. We further evaluate how well the different benchmark models can be discriminated. In IV we present our conclusions.

II. BENCHMARK MODELS AND EXPERIMENTAL CONSTRAINTS

For simplicity we assume that the WIMP is a Dirac fermion. The mediator can be either a scalar particle or a vector particle, which couples only to electrons. Extending this coupling to all leptons would be straightforward. The only place where this matters is the width of the mediator particle, which gets increased by additional couplings to muons and taus. The width is calculated using the program BRIDGE [11]. As the width turns out to be small for the coupling values considered in the following, taking for example a generation-blind scenario instead would have no relevant effect on our results.

The interaction terms appearing in the Lagrangian are denoted in Table I. Our analysis uses light mediator particles. Therefore, the momentum dependence in the propagator of the mediator plays an important role and cannot be neglected. Hence, it is not possible to formulate the results in terms of an effective dimension-six operator of the form $\bar{e}e\bar{\chi}\chi$ or $\bar{e}\gamma_\mu e\bar{\chi}\gamma^\mu\chi$ for scalar or vector mediator, respectively, where the mediator is integrated out. Nevertheless, one can still define an effective mass M_* as

$$M_* = \frac{M_\phi}{\sqrt{g_{ee\phi}g_{\chi\chi\phi}}} \quad (1)$$

as in Ref. [15]. In the limit of a heavy mediator, the term $1/M_*^2$ becomes the prefactor of the dimension-six operator.

model	mediator mass	mediator spin	WIMP mass	M_*
LSL	8 GeV	0 (scalar)	5 GeV	30 GeV
LVL	8 GeV	1 (vector)	5 GeV	30 GeV
LSH	8 GeV	0 (scalar)	120 GeV	27.4 GeV
LVH	8 GeV	1 (vector)	120 GeV	21 GeV
HSL	200 GeV	0 (scalar)	5 GeV	1250 GeV
HVL	200 GeV	1 (vector)	5 GeV	1250 GeV
HSH	200 GeV	0 (scalar)	120 GeV	332.4 GeV
HVH	200 GeV	1 (vector)	120 GeV	511.8 GeV

TABLE II: Overview of the different model scenarios used in our analysis. The first and third letter of the model name denote the mass (light or heavy) of the mediator and WIMP, respectively, while the middle one describes the spin nature of the mediator (scalar or vector).

In the following, we define 8 different model scenarios. They are characterized by three different options, namely the spin and mass of the mediator particle and the mass of the WIMP. For the spin of the mediator particle we investigate the two possibilities already mentioned, namely a scalar and a vector particle. In many scenarios the dark sector is linked to the Standard Model via kinetic mixing of a dark photon of a hidden $U(1)$ with the $U(1)$ hypercharge of the Standard-Model [36]. In the scalar case we assume that the mediator couples chiral and exclusively to electrons and WIMPs. By measuring the spin of the mediator such models can be either confirmed or disfavoured.

For the two masses we define a light and a heavy scenario each, with values of 8 GeV and 200 GeV for the mediator particle and 5 and 120 GeV for the WIMP mass.

An overview is shown in Table II together with the effective mass M_* used for each scenario. The exact choice of masses is somewhat arbitrary, but has been guided by the following considerations. The mass of the light WIMP is chosen such that it is below the typical reach of direct detection experiments, while the heavy scenario has a mass which is beyond the reach of direct searches at LEP. The two choices for the mediator mass have then been chosen such that in the light-light and heavy-heavy models the on-shell decay of a mediator particle into two WIMPs is kinematically forbidden.

The coupling parameters for the light WIMP models are already constrained by direct searches at LEP. Therefore, we choose our effective mass such that they are at the 90% CL exclusion boundary given in Ref. [15]. For the 200 GeV mediator the effective mass parameter can be taken directly from there, while for the 8 GeV mediator we have instead used the given value for the 10 GeV curve. This is slightly more restrictive than the true 8 GeV value, so with this choice we are erring on the safe side. The heavy WIMP scenarios with a WIMP mass of 120 GeV are beyond the reach of LEP. As the mediator couples only to electrons, also searches at hadron colliders cannot significantly constrain the coupling parameters. Only a direct interpretation of the WIMP as

dark matter candidate would immediately yield strong constraints by direct detection experiments [5], and in fact reduce the signal-to-background ratio to a value too low for realistic studies. Therefore, we set the couplings in the heavy WIMP cases to a value that gives similar cross sections as the corresponding light WIMP scenario. This choice also simplifies comparisons between the two options.

III. DISCRIMINATIVE OBSERVABLES

The spin of the mediator can be assessed by appealing to the analytic behaviour of the scattering amplitude dictated by Regge theory [23, 24] in the limit of large invariant mass between each produced particle compared to the propagating momentum (and any mass of fields), $s_{ij} \gg |t_i|$. In this *multi-Regge kinematic* limit, which is attained within the VBF cuts, the analytic behaviour of a $2 \rightarrow n$ scattering is determined by

$$\mathcal{M}^{p_a p_b \rightarrow p_1 p_2 p_3 p_4} \rightarrow s_{12}^{\alpha_1(t_1)} s_{23}^{\alpha_2(t_2)} s_{34}^{\alpha_3(t_3)} \gamma, \quad (2)$$

p_1, \dots, p_4 are the final state momenta ordered in rapidity, and γ depends on the couplings, the t -channel momenta t_i and ratios of $s_{ab}/(\prod s_{ij})$ only. The powers α_i determining the scaling behaviour with s_{ij} depend on the spin of the particle exchanged in the t -channel, $\alpha_i = J_i$ up to radiative corrections. In cases where the mass of the exchanged particles is negligible, the spin of the exchanged particle can therefore be inferred by studying the scaling of the cross section with the invariant mass between the electron/positron pair, see Fig. 1. Since $s_{ab} = 2p_{a\perp}p_{b\perp}(\cosh(y_a - y_b) - \cos(\phi_a - \phi_b))$, the constraint on the analytic behaviour of the scattering amplitude means that the spin of the exchanged messenger particle can be directly probed by investigating the scaling of the cross section with either the rapidity difference or the invariant mass between the electron-positron pair.

However, if the exchanged particle has a mass, which is large compared to the other scales of the process, then there will be modifications to this simple picture. Other distributions would then be consulted to differentiate the spin and the mass simultaneously.

Fig. 1 illustrates the different scaling of the cross section with m_{ee} and Δy_{ee} respectively, within our models. The predictions from the Regge analysis is observed: for a fixed setup of masses, the scalar exchange is suppressed at large m_{ee} and Δy_{ee} compared to the models with a vector mediator. While the impact of the heavy mediator mass is significant for a fixed mass of the dark matter candidate, the dominance at large Δy_{ee} of vector exchanges over scalar exchanges still holds as predicted by the Regge analysis. The same is true for $1/\sigma d\sigma/dm_{ee}$ (Fig. 2). For polarised beams and vector mediators, the S/B can reach 27% at large Δy , which is where the vector like signal processes will peak.

Conversely, scalar exchange models can get S/B enhanced by studying only regions of small Δy_{ee} .

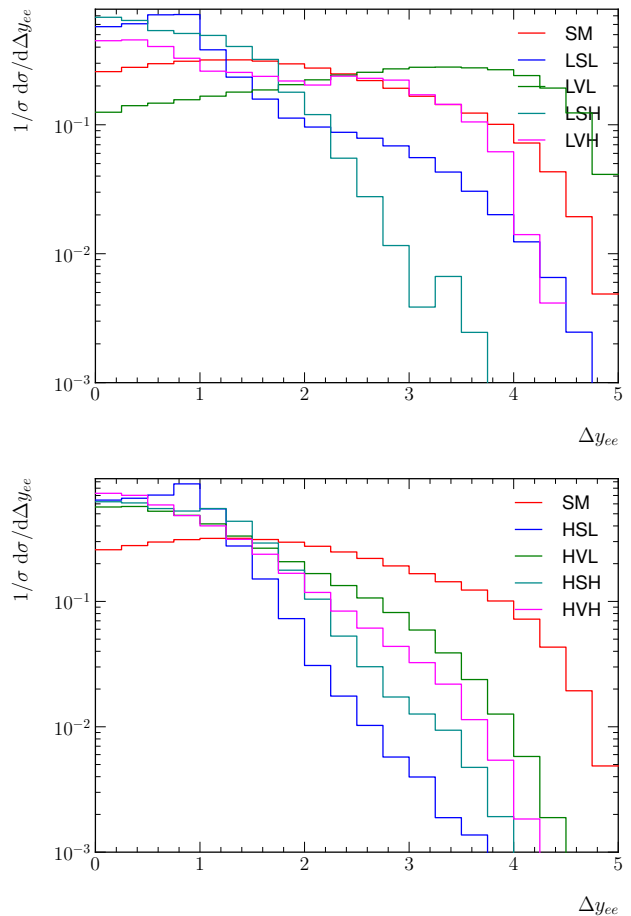


FIG. 1: $1/\sigma d\sigma/d\Delta y_{ee}$ for the standard model, and the models with light or heavy dark matter candidates and (top) a light mediator, (bottom) a heavy mediator. See text for more details.

In Fig. 3 we plot the normalised differential spectrum of the invariant mass of the invisible 4-momentum in the event. This is obviously bounded from below by the sum of the masses of the two dark matter particles. If this bound is below the mass of the mediator, then the spectrum has a pronounced peak at this mass for both scalar and vector mediators. The shape of the spectrum clearly identifies the mass-hierarchy of the mediator and DM particles: When the bound from the DM particles is above the mass of the mediator, the spectrum is very broad, as contrasted with the pronounced peak at the mediator mass.

In case we studied scalar CP-even or CP-odd WIMPs, $\Delta\phi_{e^-e^+}$ can be helpful for their discrimination. For the 8 models we study here, $\Delta\phi_{e^-e^+}$ is of minor importance.

In conclusion, the distribution of the invariant mass of the invisible momentum, M_{missing} can uniquely determine the mass scale and hierarchies of the mediator and dark matter particle, but does not discriminate between scalar and vector mediators. However, once the mass scales are determined, the spin of the mediator can be de-

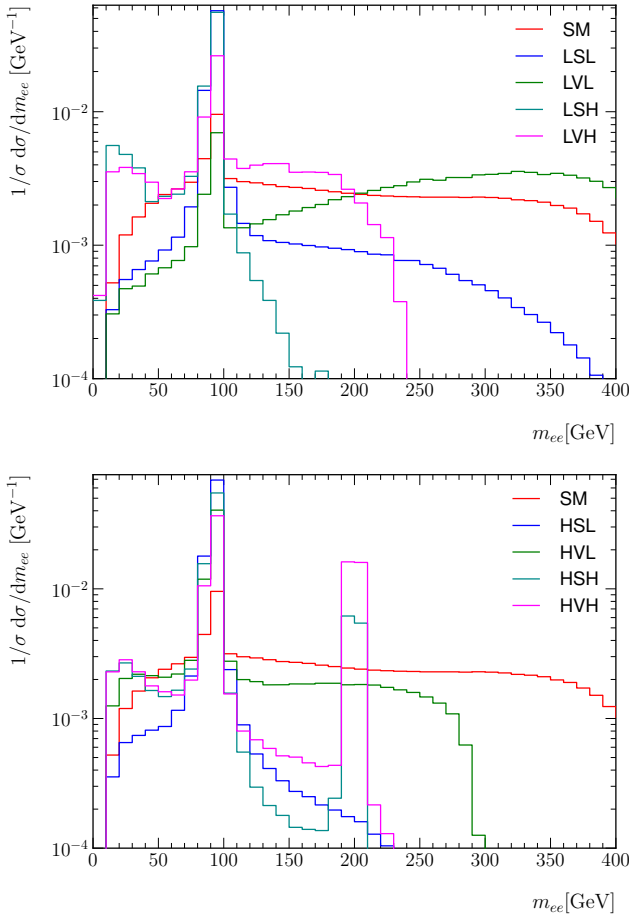


FIG. 2: $1/\sigma d\sigma/dm_{ee}$ for the standard model, and the models with light or heavy dark matter candidates and (top) a light mediator, (bottom) a heavy mediator. See text for more details.

terminated from the shape of the cross section with respect to Δy_{ee} or equivalently m_{ee} , due to the spin-dependence dictated by the Regge-analysis. Other distributions on e.g. the transverse momentum of the hardest lepton can then be used to check for consistency.

IV. DISCUSSION

As discussed in Section III we expect the observables $m_{e^+e^-}$ and the invariant mass of the WIMPS, precisely measured as recoil system of e^+e^- , to be the strongest discriminators for the benchmark models. At the ILC the lepton's energy is precisely determined and the beams can be partly polarized. We assume conservatively that the degree of polarization is 80% for the electrons and 30% for the positrons. In Table III we show the cross section for 3 different beam polarizations: unpolarized, $++$ and $+-$. The first (second) index refers to the electron (positron) beam. We find that the ratio between signal and background cross section can be improved for all

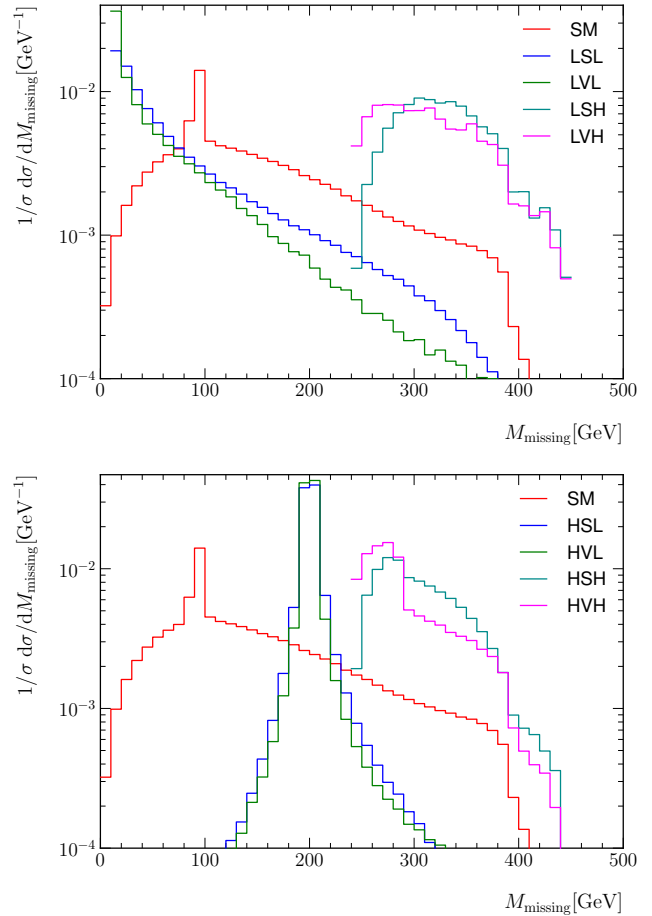


FIG. 3: $1/\sigma d\sigma/dM_{\text{missing}}$ for the standard model, and the models with light or heavy dark matter candidates and (top) a light mediator, (bottom) a heavy mediator. See text for more details.

models by using polarized beams.

Note, the signal models' cross sections respond differently to a change in the polarization of the beams. Hence the inclusive production cross section can be used to discriminate between the models as well, i.e. for scalar mediators $\sigma_{++} > \sigma_{\text{unpol}}$ while for vector mediators $\sigma_{+-} > \sigma_{\text{unpol}}$. However, in this work we will focus on the observables identified in Section III only and because of the recent interest in vector mediators [36] we will choose the $+-$ beam polarization in the following.

We perform a binned log-likelihood hypothesis test [37] using the CL_s method [38] to evaluate how well the 8 benchmark models can be discriminated from each other and from the Standard Model. For the graphs in Fig. 4 we assume only the Standard Model is realized in nature. Due to the large allowed cross section of the LVL and LVH models they can be excluded for the given coupling strength with less than 10 fb^{-1} . However, with an integrated luminosity of roughly 300 fb^{-1} all models can be disfavored at the 5σ confidence level.

For the results shown in Figs. 5-7 we assume respec-

model	σ_{unpol}	σ_{++}	σ_{+-}
SM	115.8	49.1	36.4
LSL	1.60	1.79	1.40
LVL	15.07	12.80	17.02
LSH	1.45	1.80	1.10
LVH	9.99	7.64	12.33
HSL	1.17	1.43	0.92
HVL	0.85	0.71	0.89
HSB	1.18	1.45	0.90
HVB	0.85	0.64	0.98

TABLE III: Cross sections in femtobarn for the different models imposing the constraints as outlined in the text. The three columns refer to the three different beam polarizations: averaged, ++ and +-. The first index refers to the electron beam of which we assume to be able to polarize 80% (always +). The second index represents the positron beam of which we assume to have a polarization of 30%. The cross sections vary between (0.7 – 13.0%, 1.3 – 26.1%, 2.4 – 46.8%) of the Standard Model background for three polarizations (all, ++, +-) respectively.

tively that one of the models is realized in nature, as indicated by the caption of each plot. The coupling strength in each model is chosen such that it is respecting present bounds. However, as discussed in Section II, bounds from direct and indirect detection experiments can be avoided in case the WIMPs are not stable on cosmological time scales. Only bounds from direct searches at LEP pose a stringent constraint. To evaluate how well the different quantum numbers of the benchmark models can be discriminated we assume all benchmark models have a cross section of 2.5% of the Standard Model cross section.

We have studied the impact of all the observables shown in Fig. 4, namely missing transverse energy, $m_{e^+e^-}$, $\Delta\phi_{e^+e^-}$, $\Delta y_{e^+e^-}$, p_T of the hardest lepton and

M_{missing} . We find that $m_{e^+e^-}$ and M_{missing} are sufficient to discriminate the quantum numbers of our candidate models confidently. M_{missing} gives a handle on the mass scales, while $m_{e^+e^-}$ discriminates the spin of the mediators. This is clearly demonstrated by comparing Figs. 6(c) and 6(d), where LVL and LSL are strongly discriminated by including $m_{e^+e^-}$ whereas M_{missing} has almost no discriminating power. The situation is reversed for the discrimination of LSL and LSH, as shown in Figs. 7(c) and 7(d). Here both, LSL and LSH have a pronounced peak in $m_{e^+e^-}$ at the Z boson mass (thus $m_{e^+e^-}$ is not discriminating the two models), but the large difference of the WIMP mass is reflected in $M_{\text{missing}} \geq 2M_{\text{WIMP}}$. However, if one wants to discriminate quantum numbers beyond mass and spin (e.g. CP structure) other observables should be included, e.g. $\Delta\phi_{e^+e^-}$. A combination of the variables discussed will improve the statistical significance in discriminating the models' quantum numbers.

In general and in particular for a leptophilic scenario, studying a dark sector using t-channel mediated forces is a challenging task at the LHC. This study has demonstrated that even with conservative assumptions on the level of polarization, the ILC can conclusively explore the quantum numbers of a dark sector by using a combination M_{missing} and $m_{e^+e^-}$.

Acknowledgments

MR acknowledges partial support by the Deutsche Forschungsgemeinschaft via the Sonderforschungsbereich/Transregio SFB/TR-9 “Computational Particle Physics” and the Initiative and Networking Fund of the Helmholtz Association, contract HA-101 (“Physics at the Terascale”)

-
- [1] E. Komatsu *et al.* [WMAP Collaboration], *Astrophys. J. Suppl.* **192**, 18 (2011). [arXiv:1001.4538 [astro-ph.CO]].
 - [2] P. Picozza, A. M. Galper, G. Castellini, O. Adriani, F. Altamura, M. Ambriola, G. C. Barbarino and A. Basili *et al.*, *Astropart. Phys.* **27**, 296 (2007); O. Adriani *et al.* [PAMELA Collaboration], *Nature* **458**, 607 (2009).
 - [3] M. Ackermann *et al.* [Fermi LAT Collaboration], *Phys. Rev. Lett.* **108**, 011103 (2012) [arXiv:1109.0521 [astro-ph.HE]].
 - [4] M. Aguilar *et al.* [AMS Collaboration], *Phys. Rev. Lett.* **110**, no. 14, 141102 (2013); Main results at <http://www.ams02.org/>.
 - [5] C. Savage, G. Gelmini, P. Gondolo and K. Freese, *Phys. Rev. D* **83**, 055002 (2011); J. M. Cline, Z. Liu and W. Xue, *Phys. Rev. D* **87**, 015001 (2013).
 - [6] A. Birkedal, K. Matchev, M. Perelstein, *Phys. Rev. D* **70**, 077701 (2004). [hep-ph/0403004].
 - [7] J. L. Feng, S. Su and F. Takayama, *Phys. Rev. Lett.* **96**, 151802 (2006) [arXiv:hep-ph/0503117].
 - [8] M. Beltran, D. Hooper, E. W. Kolb and Z. C. Krusberg, *Phys. Rev. D* **80**, 043509 (2009) [arXiv:0808.3384 [hep-ph]].
 - [9] Q. -H. Cao, C. -R. Chen, C. S. Li, H. Zhang, *JHEP* **1108**, 018 (2011). [arXiv:0912.4511 [hep-ph]].
 - [10] M. Beltran, D. Hooper, E. W. Kolb, Z. A. C. Krusberg, T. M. P. Tait, *JHEP* **1009**, 037 (2010). [arXiv:1002.4137 [hep-ph]].
 - [11] P. Meade and M. Reece, hep-ph/0703031.
 - [12] J. Goodman, M. Ibe, A. Rajaraman, W. Shepherd, T. M. P. Tait, H. -B. Yu, *Phys. Lett. B* **695**, 185-188 (2011). [arXiv:1005.1286 [hep-ph]].
 - [13] Y. Bai, P. J. Fox, R. Harnik, *JHEP* **1012**, 048 (2010). [arXiv:1005.3797 [hep-ph]].
 - [14] A. Rajaraman, W. Shepherd, T. M. P. Tait, A. M. Wijangco, [arXiv:1108.1196 [hep-ph]].
 - [15] P. J. Fox, R. Harnik, J. Kopp and Y. Tsai, *Phys. Rev. D* **84**, 014028 (2011) [arXiv:1103.0240 [hep-ph]].
 - [16] P. J. Fox, R. Harnik, J. Kopp and Y. Tsai, *Phys. Rev. D*

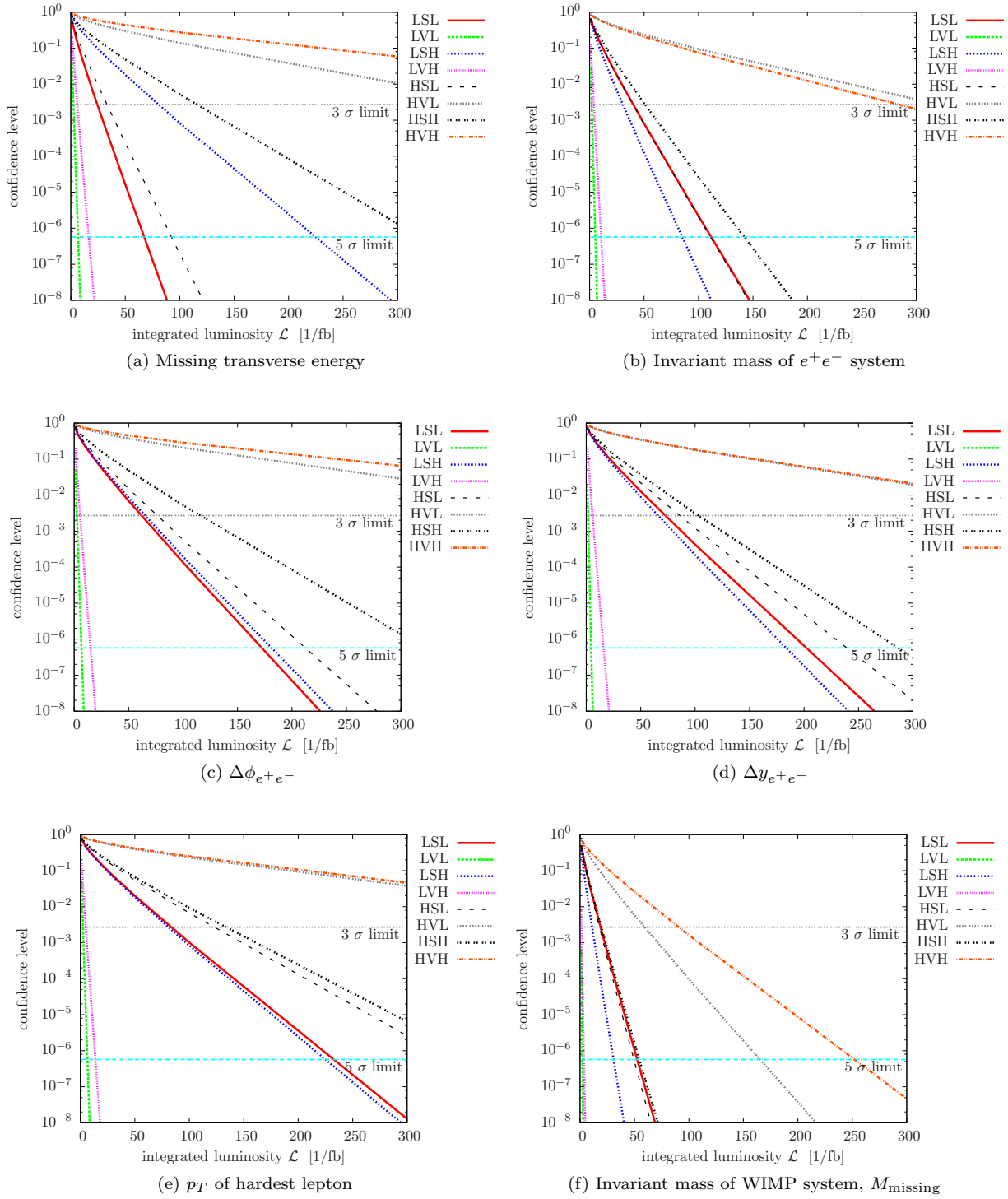


FIG. 4: Assuming realization of the Standard Model only, these plots show the confidence level to which the respective Dark Sector model can be disfavored using just one observable. The curves take into account not only the shapes but also the normalization of the model's cross section.

85, 056011 (2012).

[17] T. Plehn, D. L. Rainwater, D. Zeppenfeld, Phys. Rev. Lett. **88**, 051801 (2002). [hep-ph/0105325].

[18] G. Klamke, D. Zeppenfeld, JHEP **0704**, 052 (2007). [hep-

ph/0703202 [HEP-PH]].

[19] J. R. Andersen, K. Arnold, D. Zeppenfeld, JHEP **1006**, 091 (2010). [arXiv:1001.3822 [hep-ph]].

[20] O. J. P. Eboli, D. Zeppenfeld, Phys. Lett. **B495**, 147-154

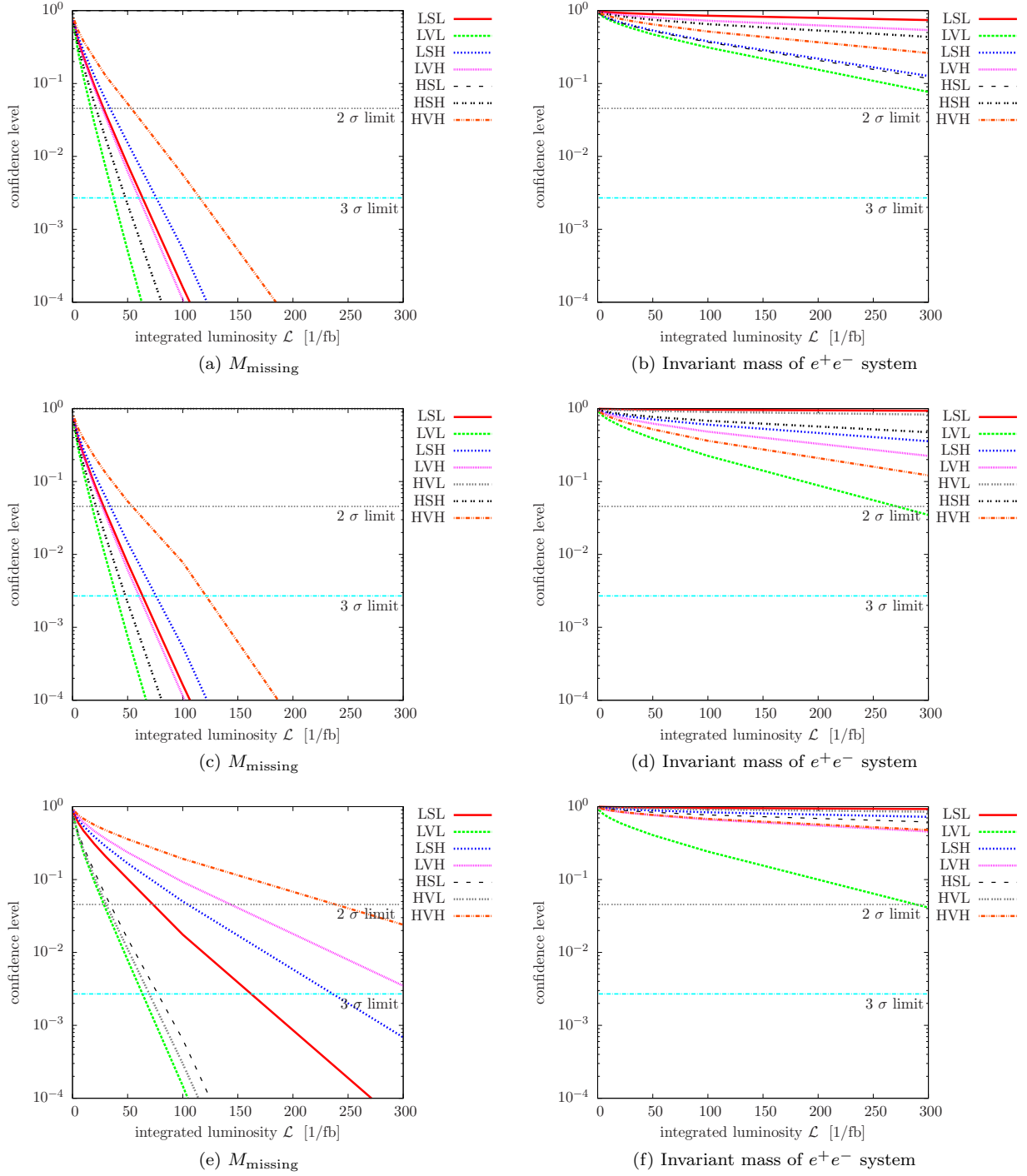


FIG. 5: The curves illustrate the level to which the M_{missing} and $m_{e^+e^-}$ can discriminate between the different models, assuming the realization of HVL (5(a)-5(b)), HSL (5(c)-5(d)) and HSH (5(e)-5(f)). All cross sections are assumed to be 2.5% of the Standard Model background cross section.

- (2000). [hep-ph/0009158].
- [21] A. J. Buras, P. Gambino, M. Gorbahn, S. Jager, L. Silvestrini, Phys. Lett. **B500**, 161-167 (2001). [hep-ph/0007085].
- [22] G. D'Ambrosio, G. F. Giudice, G. Isidori, A. Strumia, Nucl. Phys. **B645**, 155-187 (2002). [hep-ph/0207036].

- [23] T. Regge, Nuovo Cim. **14** (1959) 951.
- [24] R. C. Brower, C. E. DeTar and J. H. Weis, Phys. Rept. **14** (1974) 257.
- [25] G. Aad *et al.* [ATLAS Collaboration], JINST **3** (2008) S08003.
- [26] G. L. Bayatian *et al.* [CMS Collaboration], J. Phys. G

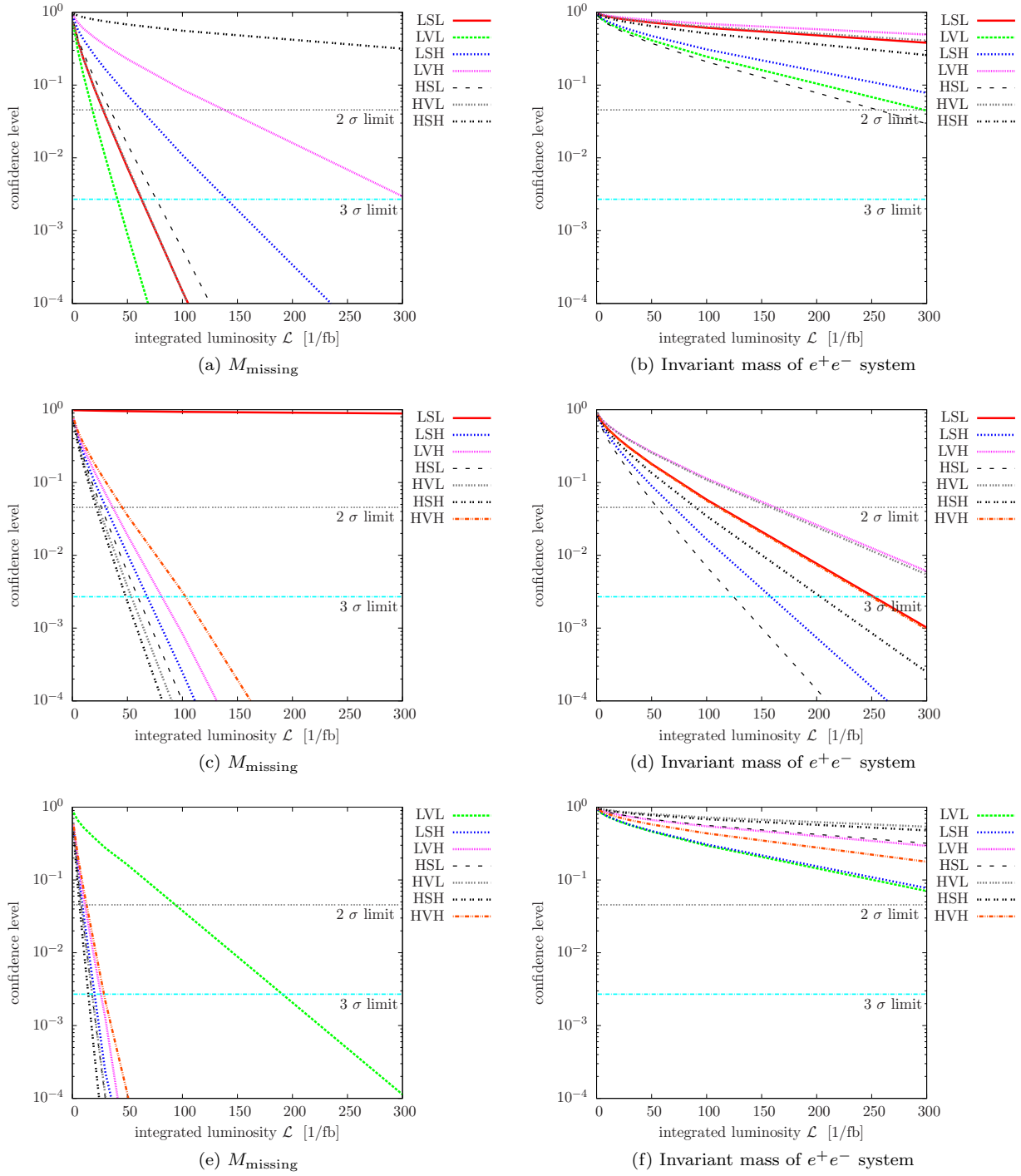


FIG. 6: The curves illustrate the level to which the M_{missing} and $m_{e^+e^-}$ can discriminate between the different models, assuming the realization of LVL (6(a)-6(b)), LSL (6(c)-6(d)) and LVH (6(e)-6(f)). All cross sections are assumed to be 2.5% of the Standard Model background cross section.

- 34 (2007) 995.
- [27] D. E. Kaplan, M. A. Luty and K. M. Zurek, Phys. Rev. D **79**, 115016 (2009) [arXiv:0901.4117 [hep-ph]].
- [28] P. J. Fox and E. Poppitz, Phys. Rev. D **79**, 083528 (2009) [arXiv:0811.0399 [hep-ph]].
- [29] M. Cirelli, M. Kadastik, M. Raidal and A. Strumia,

- Nucl. Phys. B **813**, 1 (2009) [Addendum-ibid. B **873**, 530 (2013)] [arXiv:0809.2409 [hep-ph]].
- [30] C. -R. Chen and F. Takahashi, JCAP **0902**, 004 (2009) [arXiv:0810.4110 [hep-ph]].
- [31] H. An, L. -T. Wang and H. Zhang, arXiv:1308.0592 [hep-ph].

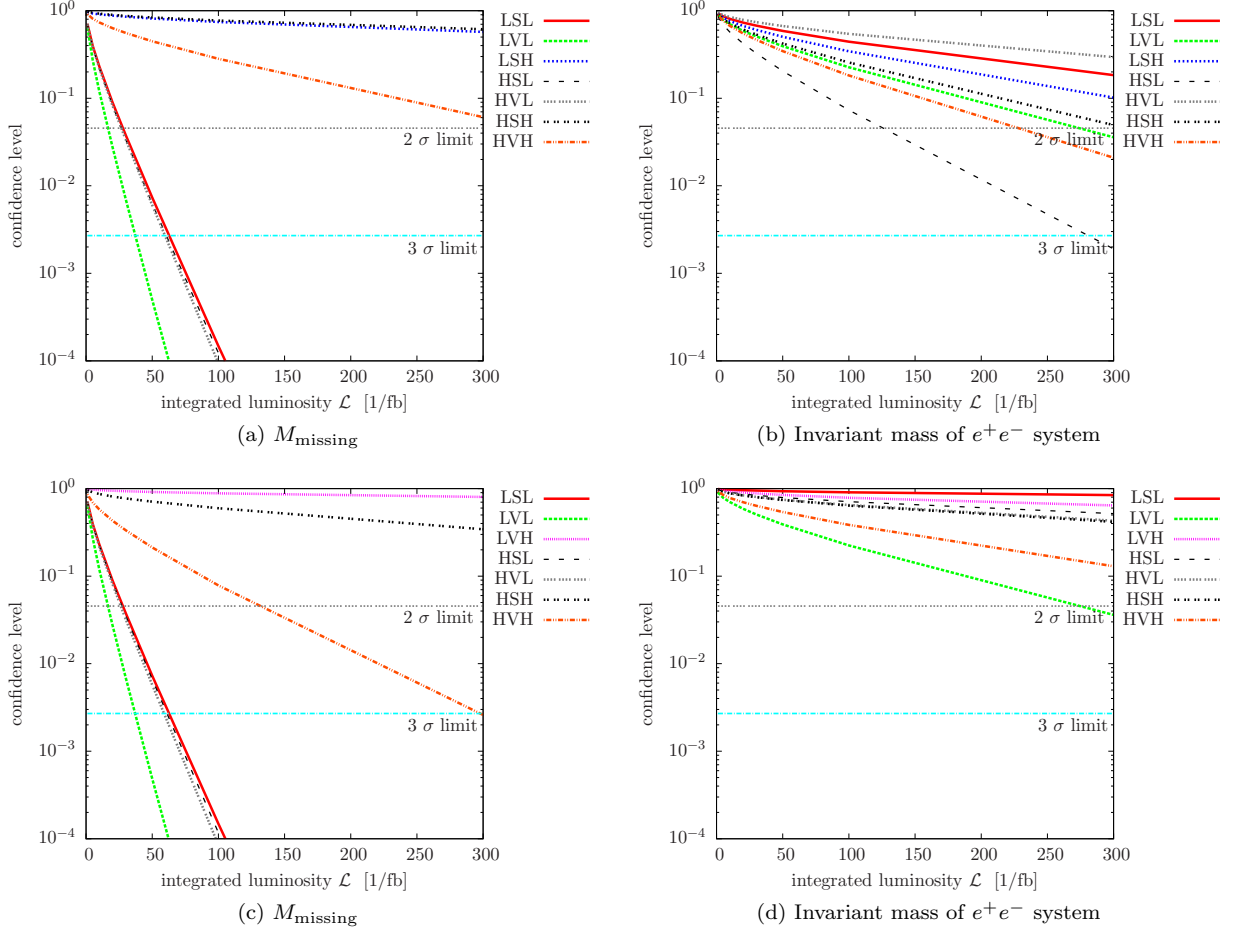


FIG. 7: The curves illustrate the level to which the M_{missing} and $m_{e^+e^-}$ can discriminate between the different models, assuming the realization of LVH (7(a)-7(b)), LSH (7(c)-7(d)). All cross sections are assumed to be 2.5% of the Standard Model background cross section.

- [32] T. Cohen and K. M. Zurek, Phys. Rev. Lett. **104**, 101301 (2010) [arXiv:0909.2035 [hep-ph]].
- [33] M. J. Strassler and K. M. Zurek, Phys. Lett. B **651**, 374 (2007) [hep-ph/0604261].
- [34] H. Dreiner, M. Huck, M. Kramer, D. Schmeier and J. Tattersall, Phys. Rev. D **87**, 075015 (2013) [arXiv:1211.2254 [hep-ph]].
- [35] ILC Technical Design Report [ILC Collaboration], <http://www.linearcollider.org/ILC/Publications/Technical-Design-Report>; G. Aarons *et al.* [ILC Collaboration], arXiv:0709.1893 [hep-ph].
- [36] B. Holdom, Phys. Lett. B **166**, 196 (1986); R. Foot and X. -G. He, Phys. Lett. B **267**, 509 (1991); S. A. Abel, M. D. Goodsell, J. Jaeckel, V. V. Khoze and A. Ringwald, JHEP **0807**, 124 (2008); N. Arkani-Hamed and N. Weiner, JHEP **0812**, 104 (2008).
- [37] T. Junk, Nucl. Instrum. Meth. A **434** (1999) 435. T. Junk, CDF Note 8128 [cdf/doc/statistics/public/8128]. T. Junk, CDF Note 7904 [cdf/doc/statistics/public/7904]. H. Hu and J. Nielsen, in 1st Workshop on Confidence Limits, CERN 2000-005 (2000).
- [38] A. L. Read, CERN-OPEN-2000-205. A. L. Read, J. Phys. G **G28** (2002) 2693-2704.